16th World Conference on Earthquake, 16WCEE 2017
Santiago Chile, January 9th to 13th 2017
Paper N° 2267 (Abstract ID)
Registration Code: S-K1464694459

DYNAMIC ANALYSIS OF THE SEISMIC BEHAVIOR OF A BASE-ISOLATED CONTAINER CRANE DURING THE 2011 OFF THE PACIFIC COAST OF TOHOKU EARTHQUAKE

E. Kohama [1], T. Sugano[2]

[1] Head, Earthquake and Structural Dynamics Group, Port and Airport Research Institute, kohama-e83ab@pari.go.jp
[2] Coastal Development Institute of Technology, t_sugano@cdit.or.jp

Abstract

Earthquake-resistant technologies have improved, e.g., with the introduction of seismic base isolation, since many container cranes for loading and unloading vessels were damaged during the 1995 Southern Hyōgo Prefecture Earthquake. The developed container cranes were installed to high earthquake-resistant quays and have contributed significantly to maintaining the function of the container terminal after large earthquakes. In relation to seismic performance verification of container cranes, strong earthquake motions have been observed at some container cranes in ports in Japan. Records of strong earthquake motion at a base-isolated container crane and the underlying wharf during the 2011 off the Pacific coast of Tohoku Earthquake were examined in detail to clarify the seismic properties of the container crane. Taking account of modeling of the base isolation system, a series of dynamic response analyses were conducted to reproduce the observed seismic behavior of the crane in this study.

The latter half of the acceleration time history in the traverse direction, calculated by the crane model without seismic isolation, was not consistent with the observed acceleration during the earthquake. On the other hand, the acceleration history calculated by the crane model in which seismic isolation was always operational was smaller than the observed value as a whole. In the case where the seismic isolations in the four leg portions of the crane work individually by breaking of each shear pin, the calculated acceleration showed good agreement with the observed acceleration. The importance of this precise modeling of the isolation system was recognized from these results.

Comparison between the calculated and observed acceleration showed good agreement in the traveling direction of the crane, which was different from the direction of motion of seismic isolation. The observed vertical acceleration of the crane, including high-frequency components, showed less agreement with the calculated acceleration. There were differences in components higher than 2 Hz in the Fourier spectrum between the observed and calculated acceleration. The strong motion seismograph is not installed directly to the main structure of the crane but in the machine chamber. Accordingly, the installation location of the seismograph was considered to influence the high-frequency components of the acceleration wave.

Keywords: container crane; strong-motion earthquake observation; seismic response analysis

1. Introduction

Since the 1995 Southern Hyōgo Prefecture Earthquake, when many container cranes for loading and unloading vessels were damaged, earthquake resistance technologies have improved, e.g., with the introduction of seismic base isolation.[1, 2, 3] The developed container cranes were installed on high earthquake-resistant quays and contribute significantly to maintaining the function of the container terminal after large earthquakes.

In relation to seismic performance verification of container cranes, earthquake strong motion observations have begun at some container cranes in Japanese ports. Strong motion earthquake records observed at a base-isolated container crane and the underlying wharf during the 2011 off the Pacific coast of Tohoku Earthquake were examined in detail to clarify the seismic properties of the container crane.[4] Dynamic analysis with the three-dimensional finite element method is often performed for seismic performance verification of base-isolated container cranes.[5, 6] However, there have been no studies in which the accuracy of modeling and results of the analysis were validated with actually observed seismic behavior of container cranes. Here, a series of dynamic response analyses taking account of modeling of the base isolation system were conducted to reproduce the observed seismic behavior of the crane, and differences between the observations and analysis results are discussed.

2. Container Crane and Analysis Model

An actual container crane with a seismic isolation device installed on a jacket pier was examined in this study. Strong seismic motion observations have been performed on the crane, the pier, and the ground, as shown in Figure 1. The seismometer on the crane is installed on the landward end of the machine room. Four seismic base isolation mechanisms are mounted on four traveling devices on the leg portion of the crane to reduce vibration in the traverse direction, which is the same as the orthogonal direction relative to the face line of the jacket pier. The isolation consists of swivel bearings, a restoring mechanism, and a damping mechanism. A shear pin fixing movement of the swivel bearings under normal conditions ruptures during large earthquakes, thus initiating the isolation.

Strong seismic motion of > 200 Gal was recorded on the observed crane during the 2011 off the pacific coast of Tohoku Earthquake. Based on reports by people working at the pier and the crane after the earthquake, the crane was loading and unloading cargo with the boom in the down position during the earthquake, and base isolation was running due to fracturing of the shear pins.

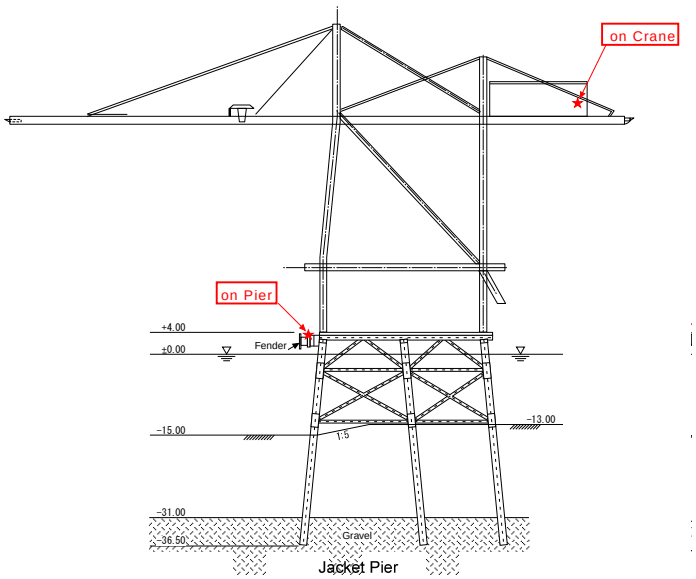

Fig. 1 – Container crane and seismometer arrangement

The crane with the boom in the down position, similar to the state at the time of the earthquake, was modeled in three dimensions using the general finite element analysis program, NASTRAN (see Figure 2). As it is difficult to determine where the trolley was at the time of the earthquake, it was placed at the most seaward side of the boom (outreach). Primary structural components of the crane were modeled by elastic beam elements; bending and axial stiffness and density were set by calculation based on Young's modulus, cross-sectional area, second moment of area, and weight of each component. Elements are color coded in Figure 2. A pin joint or a rigid joint not allowing rotation was introduced to each connection point of the components according to the joining structure. Pin joints were employed at the end of the tension bars linking the boom to the upper support, and the end of the diagonal brace linking the seaward and landward legs. Annexed equipment other than the main structural components consisted of the machine chamber, traveling device, trolley, spreader, etc., and their total mass of 1127 t was modeled as mass points. Stiffness proportional damping of 2.5% in damping ratio was used, calculating the primary eigenmode in the traverse direction by eigenvalue analysis as described later.

The peripheral part of the traveling device was modeled as shown in Figure 3. The traveling devices were modeled as lumped masses, and lift and slip between the traveling device and the rail were represented by a gap element, i.e., a non-linear spring element incorporated in NASTRAN. The spring constant of the gap element is inferior in tension and was employed to represent the lift of the wheels. The spring constant in compression was assigned a huge value as the wheels are in contact with the rail. The friction coefficient was set to the cap element to consider wheel slippage; the wheels slip when the frictional force exceeds a certain resistance. The wheels were thought to be braked as the crane was handling cargo during the earthquake. Thus, there was no rotation of the wheels, and only their slippage on the rails was taken into account in the model. The spring constant of the gap element in compression was set to 10 times as large as the adjacent element, with reference to previous research.[5] The spring constant in tension was set to 1/1000 of the element with the lowest stiffness.

Four seismic isolation devices consisting of a spring (restoring mechanism), a damper (damping mechanism), and swivel bearings are installed between the traveling device and the crane body (see

Figure 4). The spring coefficient and damping constant in modeling of the isolation device were set to 785 kN/m and 500 kNs/m, respectively, based on a previous study.[7] Only the rotation around two vertical (z) axes was set to be free in modeling of the swivel bearings, as shown in Figure 3. The seismic response calculation was conducted with a default value of 500 kN in breaking load of the shear pins acting as trigger mechanism, with reference to the previous study.[7]

The results of calculating the position of the center of gravity for the analysis model are shown in Figure 5. The center of gravity of the model was positioned 6.34 m in the horizontal direction and 32.96 m in the vertical direction from the top of the seaward rail.

The results of eigenvalue analysis for the model are illustrated in Figure 6. The eigenvalues of the non-isolated crane in which the isolation mechanism is not operational are shown. The third to fifth modes are illustrated, and the primary and secondary modes are omitted as it is the swing of the spreader. The third and fourth modes were vibration modes in the traveling direction (the direction normal to the jacket pier face line) and their natural frequencies were 0.243 Hz and 0.386 Hz, respectively. The vibration mode in the traverse direction (the direction parallel to the jacket pier face line) was the fifth mode the natural frequency of which was 0.484 Hz. This result corresponds approximately to the dominant frequencies of the amplification ratio in the Fourier spectrum of the crane to the jacket in the earthquake observation.[4]

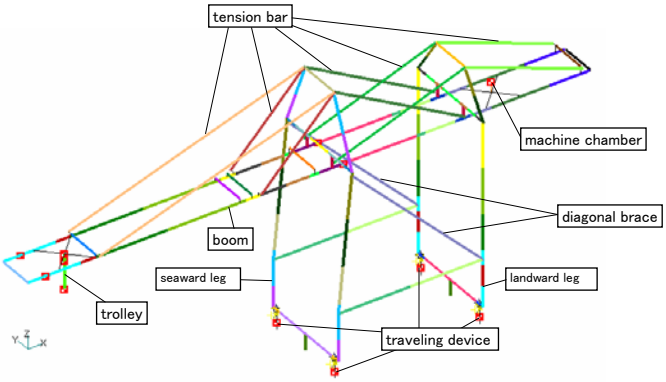

Fig. 2 – Analysis model

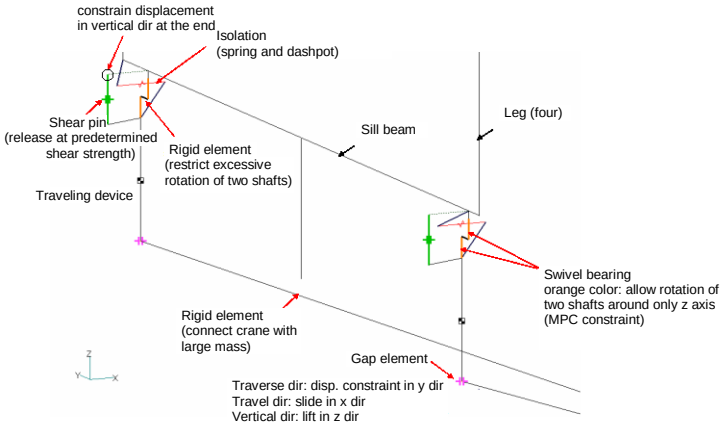

Fig. 3 – Modeling around traveling device

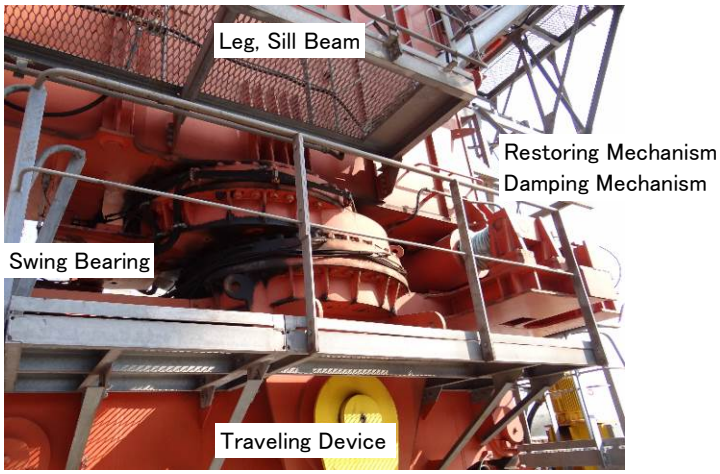

Fig. 4 – Base isolation mechanism

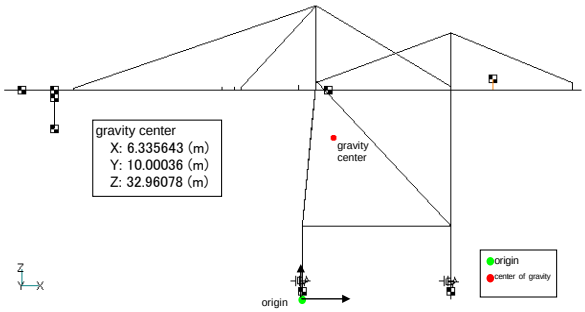

Fig. 5 – Center of gravity position

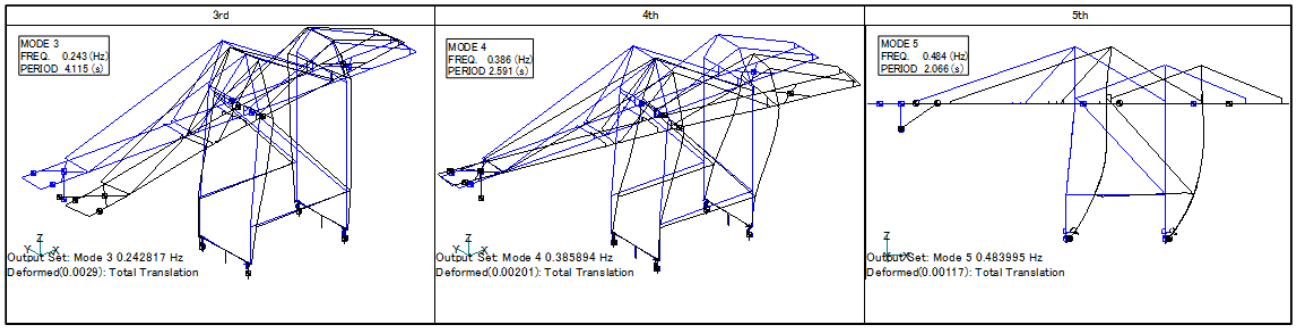

Fig. 6 – Eigenvalue analysis

3. Analysis Results

In the analysis to represent the dynamic behavior of the container crane during the 2011 off the Pacific coast of Tohoku Earthquake, the observed seismic waves on the jacket pier in the vertical and horizontal directions were employed as input waves to the crane model (see Figure 7). The acceleration time history recorded by the strong motion seismograph in the machine chamber of the crane was compared with the analysis results. The analysis cases shown in Table 1 were examined considering the

vibration characteristics of the crane and the operation of seismic isolation. Focusing on the traverse direction in which the isolation is operational, comparisons between the observations and the analysis are shown in Figures 8 and 9: acceleration time history and its Fourier spectrum in the location of the seismograph on the crane in each analysis case. The Fourier spectra were smoothed with a Parzen window of 0.05 Hz in the band width.

The analysis results of Case-N1 in which isolation was not operational underestimated the first half of the observed acceleration on the crane in the traverse direction and overestimated the second half (see Figure 8(a)). On the other hand, the results of Case-I with isolation operational underestimated the whole history of the observed acceleration (see Figure 8(c)). The seismic isolation, which was always operational in Case-I, began to operate by breaking the shear pins during earthquakes. Therefore, in Case-IM1 considering the shear pins, the isolation began to work when shear force exceeded the rupture strength of the pins. The timing of shear pin rupture was different in each of the four isolation devices on traveling devices as simultaneous seismic input in the three directions was applied to the analysis model. Isolation was engaged first in the right seaward leg under the conditions used in this study (see Figure 10). The first half of acceleration in the traverse direction calculated in Case-IM1 showed better agreement with the observed acceleration than Case-I in which isolation was always operational (see Figure 8(d)). However, as the first half of the acceleration was still underestimated in Case-IM1, a larger rupture strength of the shear pins was taken into account in Case-IM2 and Case-IM3 not to actuate the isolation under larger excitation. As dominant frequencies of Fourier spectra of the acceleration in Case-N1 and Case-IM1 were higher than the observed acceleration, we also attempted to reduce the natural frequency of the model without isolation. This is because, in modeling of the container crane, there is the potential for the natural frequency to be lower than expected due to overlooking the mass of stiffeners and attachments other than the main structures and play of bearings during strong excitation. In this study, as it was difficult to reduce the stiffness considering the play of the bearings, the mass of the model components was increased across the board such that the natural frequency in the traverse direction of the model without isolation was adjusted to 0.466 Hz. In Case-N2 in which only adjustment of the natural frequency was performed for the model without isolation, acceleration was overestimated at around 120 s and later (see Figure 8(b)) but the dominant frequency in the Fourier spectrum of the acceleration of around 0.45 Hz showed better agreement with the observations than Case-N1 (see Figure 9(b)).

In Case-IM2 and Case-IM3 considering the increase in rupture strength of the shear pins, the calculated acceleration corresponded better to the observations than Case-IM1 in which the rupture strength was 500 kN (see Figure 8(e, f)). In particular, the calculated acceleration at around 115 s where the amplitude of the acceleration was larger showed the best agreement with observations in Case-IM3 in which the rupture strength had a large value of 700 kN. Unlike Case-IM1 in which seismic isolation began to work at around 105 – 115 s, rupture of the shear pins concentrated at the time when acceleration was large (see Table 2). The rupture strength of 500 kN in Case-IM1 was quoted from the previous investigation[7] and the nominal strength of the shear pins may be different from the actual strength. For safety, the actual strength of material used in normal structural design is usually higher than the nominal strength. However, a greater actual strength of shear pins in the isolation mechanism would prevent the pins from fracturing as expected and thus allow large vibrations to be transmitted to the main body of the crane.

The acceleration time histories and their Fourier spectra of the crane in the traveling and traverse directions in Case-IM3 are shown in Figures 11 and 12. The acceleration in all analysis cases in the traveling direction, which is different from the direction of motion of the isolation mechanism, corresponded to the observed acceleration as well as in Case-IM3. The observed acceleration waveform in the vertical direction included large amounts of high-frequency components and did not coincide

well with the calculated waveform. The observed and calculated Fourier spectra in all directions were different in components higher than 2 Hz (see Figures 9 and 12). As the seismograph on the container crane is located in the machine chamber and is not installed directly on the main structure, the high-frequency components of the observed acceleration are thought to include local vibrations in the surrounding portion of the installed seismograph. The main components of the crane were considered in the analysis model and the observed Fourier spectra below 2 Hz are recognized as representing the properties of the main crane structure.

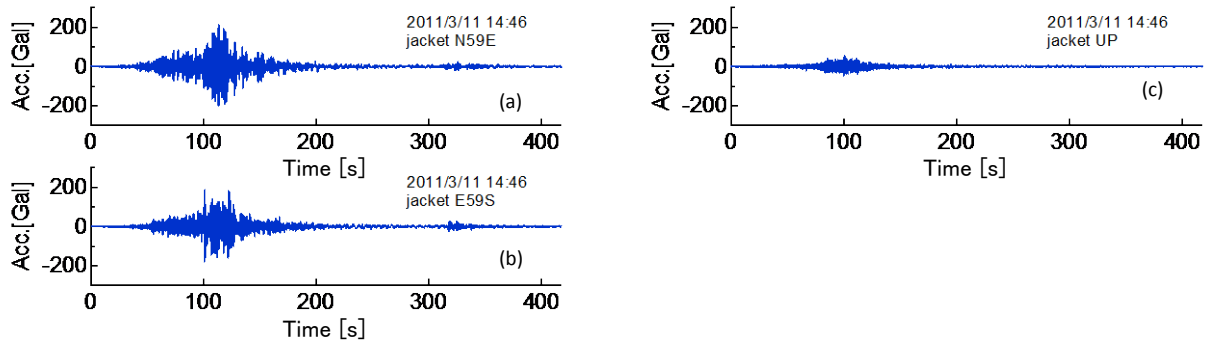

Fig. 7 – Observed acceleration time history

Table. 1 – Cases

Case	Base isolation	Considering shear pins	Vibration property
Case-N1	Not operational	–	–
Case-N2	Not operational	–	Adjusting natural period
Case-I	Operational	No	–
Case-IM1	Operational	Rupture strength 500 kN	–
Case-IM2	Operational	Rupture strength 650 kN	Adjusting natural period
Case-IM3	Operational	Rupture strength 700 kN	Adjusting natural period

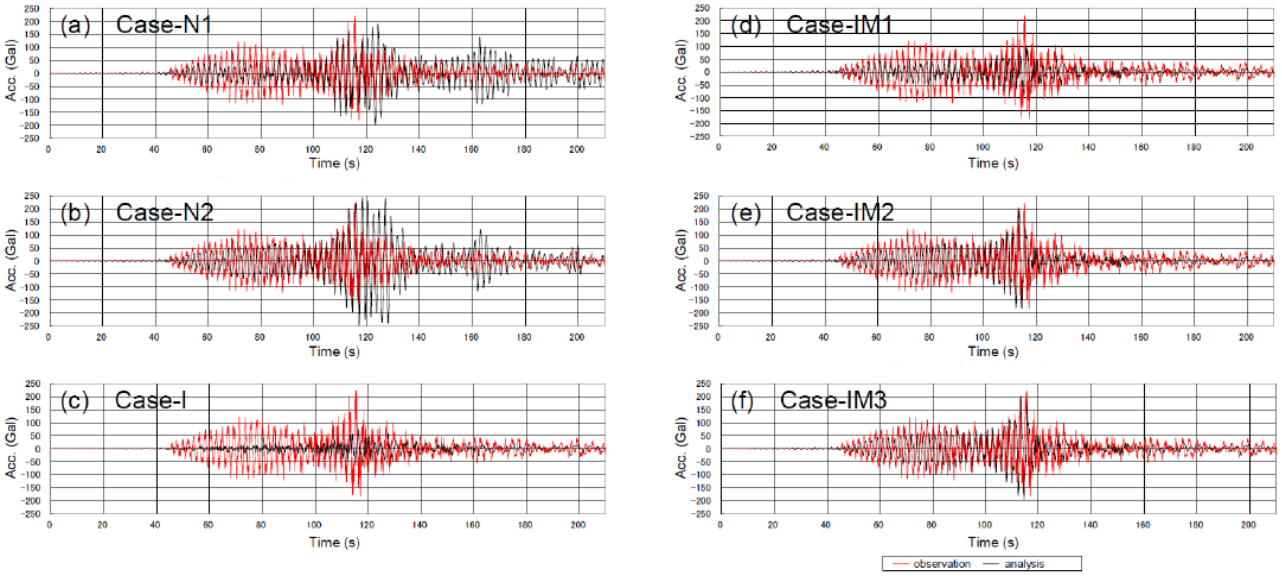

Fig. 8 – Acceleration time history in the traverse direction at the seismometer position on the crane

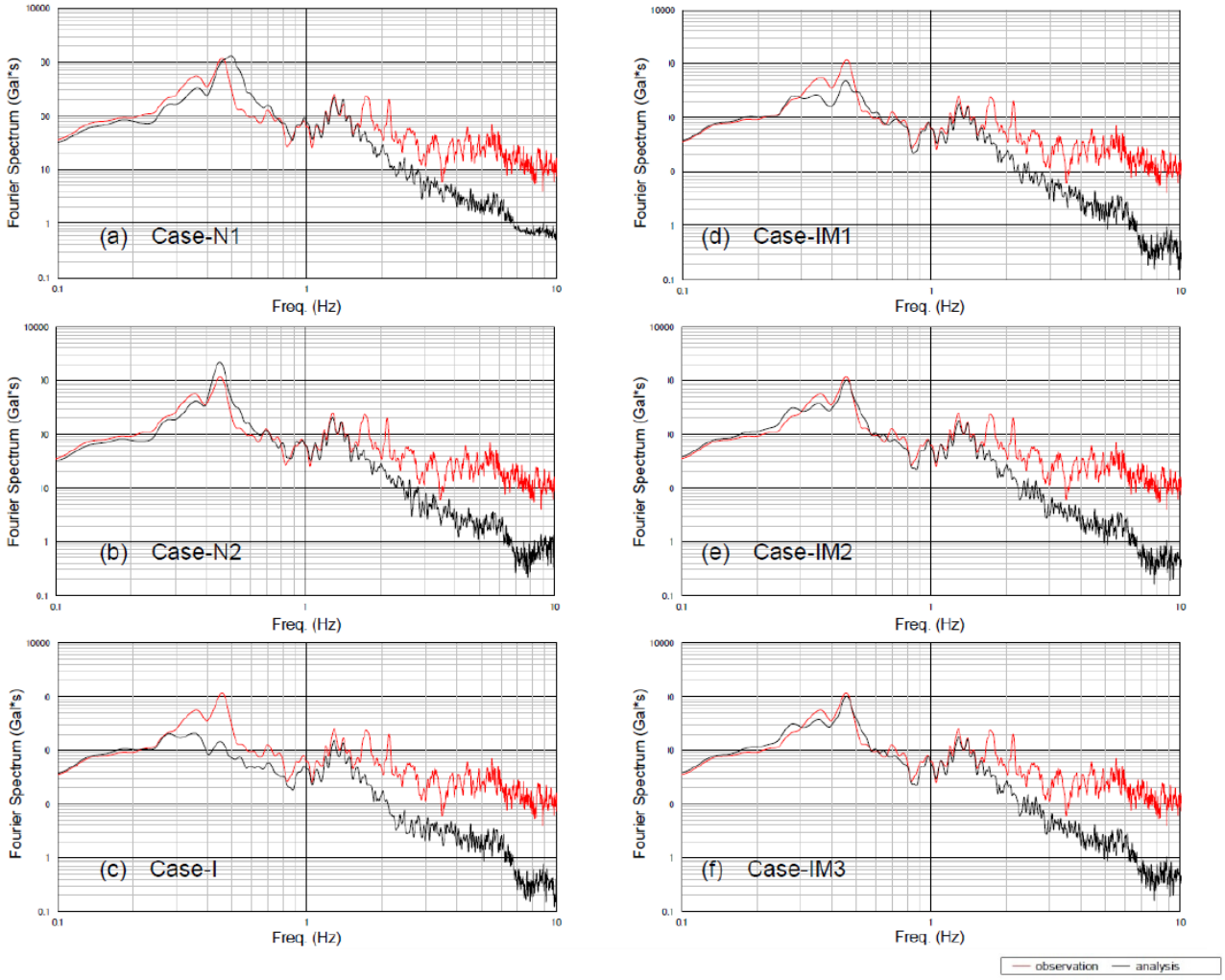

Fig. 9 – Fourier spectrum of acceleration in the traverse direction at the seismometer position on the crane

Table. 2 – Rupture time of shear pins

Case	Rupture strength	Rupture time of shear pins (s)			
		Right seaward leg	Left seaward leg	Right landward leg	Left landward leg
Case-IM1	500 kN	105.05	106.49	115.88	115.95
Case-IM2	650 kN	114.41	114.51	115.72	115.79
Case-IM3	700 kN	115.62	115.50	115.58	115.65

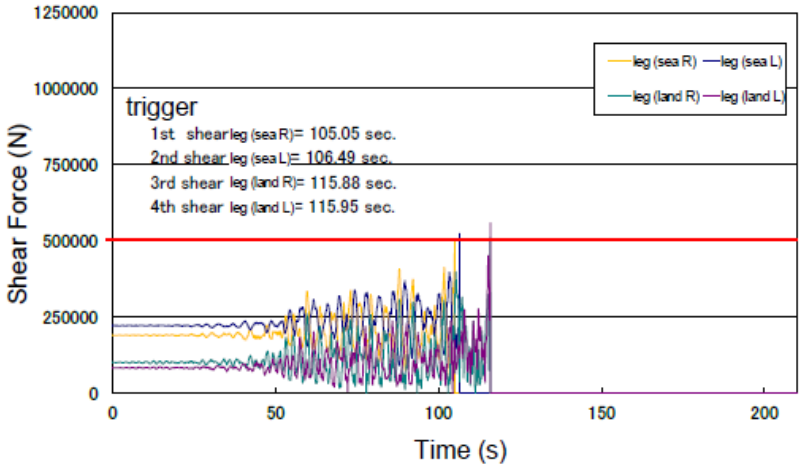

Fig. 10 – Setting rupture time considering shear force on the shear pins

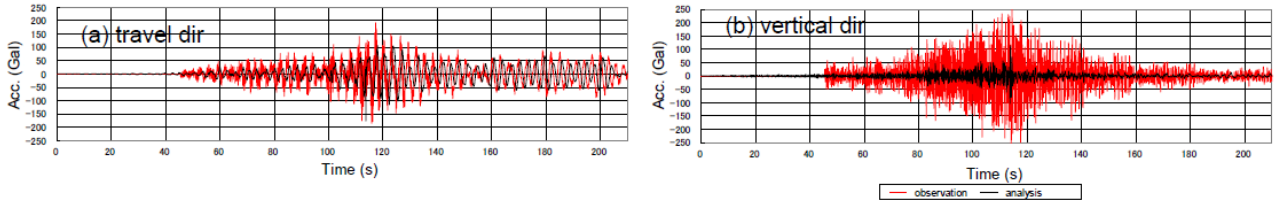

Fig. 11 – Acceleration time history in the travel and vertical directions at the seismometer position on the crane

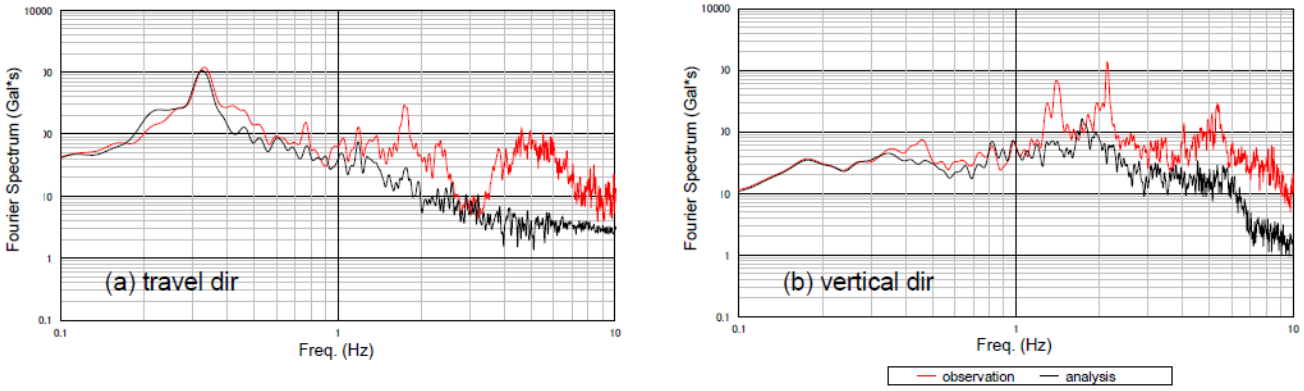

Fig. 12 – Fourier spectrum of acceleration in the travel and vertical direction at the seismometer position on the crane

4. Concluding Remarks

In this study, a series of dynamic response analyses were conducted to reproduce the observed seismic behavior of the base-isolated container crane during the 2011 off the Pacific coast of Tohoku Earthquake and the following conclusions were drawn.

− The latter half of the acceleration time history in the traverse direction, calculated by the crane model without seismic isolation, was not consistent with the observed acceleration during the earthquake. On the other hand, the acceleration history calculated by the crane model in which seismic isolation was always operational was smaller than the observations. In the analysis with seismic isolation in four leg portions of the crane operating individually by breaking of each shear pin, the calculated acceleration showed good agreement with the observations. These results indicated the importance of this precise modeling of the isolation system.

− Comparison between the calculated and observed acceleration showed good agreement in the traveling direction of the crane, which was different from the motion direction of the seismic isolation. The observed vertical acceleration of the crane including high-frequency components showed less agreement with the calculated acceleration. Differences appeared in components higher than 2 Hz in the Fourier spectrum between the observed and calculated acceleration. The strong motion seismograph is not installed directly in the main structure of the crane but in the machine chamber. Accordingly, it was considered that the installation location of the seismograph influences the high-frequency components of the observation acceleration wave.

5. References

[1] Yamamoto S, Satoh E, Nakayama Y, Sugano T, Tanabe T (2001): The shaking table test of the response controlled container crane, *Doboku Gakkai Ronbunshu*, 2001 (693), VI-53, 131-144 (in Japanese).

[2] Nakayama Y, Sugano T, Tanabe T, Satoh E, Yamamoto S, Tanaka S (2001): Experiment on behavior of response controlled container cranes under strong earthquakes, *Technical Note of the Port and Harbour Research Institute*, No. 981 (in Japanese).

[3] Sugano T, Shibakusa T, Fujiwara K, Tokunaga K, Makimoto Y, Fujiki T (2003): Study on the seismic performance of container crane –development of the container crane with isolation system–, *Report of the Port and Airport Research Institute*, **42** (2), 221-250 (in Japanese).

[4] Kohama E, Sugano T, Takenobu M, Miyata M, Nozu A (2013): Strong-motion earthquake observation of pile-supported wharves and a container crane during the 2011 off the Pacific coast of Tohoku Earthquake, *Journal of Japan Society of Civil Engineers*, Ser. B3 (Ocean Engineering), **69** (2), I_149-I_154, (in Japanese).

[5] Miyata M, Takenobu M, Nozu A, Sugano T, Kohama E, Kubo T (2009): Study on the seismic performance-based design methods for container cranes (part 2), *Technical Note of National Institute for Land and Infrastructure Management*, No. 540 (in Japanese).

[6] Miyata M, Yoshikawa S, Takenobu M, Sugano T, Kohama E, Kubo T (2010): Study on the seismic performance-based design methods for container cranes (part 3), *Technical Note of National Institute for Land and Infrastructure Management*, No. 563 (in Japanese).

[7] Okubo Y, Abiru H, Harada H, Ikeda H, Onuki Y (2000): The container crane utilizing base isolation mechanism, *The Transportation and Logistics Conference*, No. 00-50, 57-60, Japan Society of Mechanical Engineers, (in Japanese).